Research paper

Anti-obesity effects of chondroitin sulfate oligosaccharides from the skate *Raja pulchra*

Wen Li[a]*, Taishi Kobayashi[a], Syoichi Moroi[a], Hiroki Kotake[a], Tomokazu Ikoma[a], Hiroki Saeki[b], Kazuhiro Ura[b], Yasuaki Takagi[b]

[a] *Graduate School of Fisheries Sciences, Hokkaido University, 3-1-1 Minato-Cho, Hakodate, Hokkaido 041-8611, Japan*

[b] *Faculty of Fisheries Sciences, Hokkaido University, 3-1-1 Minato-Cho, Hakodate, Hokkaido 041-8611, Japan*

E-mail addresses: fenzhongbahe@outlook.com (W Li), t-hand-895ce@docomo.ne.jp (T Kobayashi), s.moroichi@gmail.com (S Moroi), kotakehiroki1146@gmail.com (H Kotake), tomo.ik.519@gmail.com (T Ikoma), saeki@fish.hokudai.ac.jp (H Saeki), kazu@fish.hokudai.ac.jp (K Ura), and takagi@fish.hokudai.ac.jp (Y Takagi)

*Corresponding author

Tel./fax: +81 138 40 5551

Abstract

We aimed to investigate the anti-obesity effects of chondroitin sulfate (CS) oligosaccharides obtained from cartilage of the skate *Raja pulchra* and to compare them with those of CSs of other molecular weights (MWts) (skate CS polysaccharides) and origins (shark CS, bovine CS). CSs suppressed pancreatic lipase activity as well as proliferation and lipid accumulation in mature adipocytes. Higher MWt CS had a greater lipase inhibitory activity than lower MWt CS. CSs of different origin show differing potencies for lipase inhibition and effects on adipocytes. Also, dietary intake of skate CS oligosaccharides could ameliorate obesity in high-fat diet mice model: it prevented gaining in body weight, liver weight and adipose tissue weight, maintained lower food consumption, inhibited intestinal absorption of triglyceride, and adjusted the serum endotoxin level. In conclusion, skate CS oligosaccharides have an anti-obesity activity, and the MWt and origin of the CSs may affect this activity.

Keywords: skate, processing waste, chondroitin sulfate, lipase, adipocyte, high-fat diet mice model

Chemical compounds studied in this article

Orlistat (PubChem CID: 3034010); para-nitrophenyl phosphate (PubChem CID: 4686862); Dimethyl sulfoxide (PubChem CID: 679); Endotoxin (PubChem CID:

53481793); Dexamethasone (PubChem CID: 5743); 3-isobutyl-1-methylxanthime (PubChem CID: 3758); Insulin (PubChem CID: 16131099)

1. Introduction

Chondroitin sulfate (CS) is a polysaccharide chain consisting of a repeated disaccharide unit composed of glucuronic acid (GlcA) and N-acetylgalactosamine (GalNAc). It is a ubiquitous component of the cell surface and extracellular matrix (Hashiguchi et al., 2011; Kwok, Warren, & Fawcett, 2012). The different types of sulfation of the disaccharide subunits lead to the generation of distinct types of CS. For example, sulfation at C-4 of GalNAc is present in CS-A and sulfation at C-6 of GalNAc is present in CS-C (Kwok, Warren, & Fawcett, 2012). CS has multiple biological effects, including anti-angiogenic (Kobayashi, Kakizaki, Nozaka, & Nakamura, 2017), immunological activity (Melgar-Lesmes et al., 2015), and neurite outgrowth-promoting activity (Hashiguchi et al., 2011). The potency of CS with regard to each of these depends on their type and molecular weight (MWt), which varies according to their origin and methods of production and purification (Martelpelletier, Farran, Montell, Vergés, & Pelletier, 2015; Volpi, 2007). Several types of CS have been isolated from various natural sources, including terrestrial vertebrates and marine species, such as cows, pigs, chickens, sharks, and skates.

Recently, a new anti-obesity bioactivity of salmon nasal CS has been reported (Han et al., 2000). Obesity is a key component of metabolic syndrome and is a

67 growing threat to public health. It usually results from an imbalance in energy intake
68 and consumption, (Zhang & Lu, 2012), and therefore inhibition of the intestinal
69 absorption of dietary fats is one of the most effective ways of treating obesity.
70 Pancreatic lipase (EC3.1.1.3) plays a key role in the digestion of 50%–70% of dietary
71 fat (Garza, Milagro, Boque, Campión, & Martínez, 2011). Therefore, inhibition of this
72 enzyme would reduce intestinal fat absorption, making it a potential target for the
73 treatment of obesity. Han et al (2000) showed that salmon nasal CS inhibits lipase
74 activity *in vitro* and that oral administration results in lower fat storage in mice fed a
75 high-fat diet.

76 Another effective way of preventing or ameliorating obesity is to inhibit fat
77 storage, and the regulation of adipocyte proliferation, differentiation, and metabolism
78 is crucial for this purpose. However, prior studies of the effect of CS in adipocytes
79 have been limited to evaluating the effect of one type of CS only, fucosylated CS from
80 sea cucumbers (Xu et al., 2015).

81 Skate fishery is one of the most important industries in northern Hokkaido.
82 However, because only the fins of the skate are used for food, a massive volume of
83 waste material is generated by the skate processing industry, which is associated with
84 serious economic loss. The cartilaginous skate head and axial skeleton, which are
85 presently discarded, are rich in CS, and this represents an attractive source of this
86 substance, because the traditional sources (bovine, porcine, and chicken cartilage) are
87 associated with concerns about zoonoses, such as bovine spongiform encephalopathy
88 and swine flu (Murado, Fraguas, Montemayor, Vázquez, & González, 2010). In

addition, Squaliformes sharks, another new source of CS, have keratan sulfate as their glycosaminoglycan, whereas most skates only contain CS (Murado et al., 2010). Thus, skate CS is easier to purify than shark CS. Moreover, shark catches are decreasing worldwide, probably owing to over-fishing (FAO, International Plan of Action for Conservation and Management of Sharks, 2014). Thus, if useful bioactivity of skate CS can be demonstrated, waste from the skate food-processing industry will become valuable.

The absorption of CS polysaccharides from the digestive system is generally very low (Yamada, Matsushima, Ura, Miyamoto, & Sugahara, 2013). However, recently, we found that CS oligosaccharides prepared from skate CS could be effectively absorbed from the intestine of rats (unpublished observation). Thus, orally administered CS oligosaccharides may be able to influence adipocyte proliferation, differentiation, and metabolism. Moreover, a new, low-cost method using a subcritical water microreaction system to produce skate CS oligosaccharides has been developed (Yamada et al., 2013). Thus, oral administration of skate CS oligosaccharides is now possible and may be beneficial for obesity.

In this study, we obtained CS oligosaccharides from the head and axial cartilages of the skate *Raja pulchra*, a major catch in northern Hokkaido, and investigated their anti-obesity effects *in vitro* and *in vivo*. Their lipase- and adipocyte- inhibitory effects were also compared with those of CSs of other MWts and origins. We hypothesized that intestinally absorbable skate CS oligosaccharides have stronger adipocyte-inhibitory activity and a weaker lipase-inhibitory activity than high MWt

CS polysaccharides; and that CSs of different origin have differing anti-obesity potencies.

2. Materials and Methods

2.1. Materials

CS polysaccharides from skate cartilage (big CS, purity 70%) and its oligosaccharides, containing 2–14 sugar units (nano CS, purity 80%), were obtained from Marukyo Bio Foods Co. Ltd. (Wakkanai, Hokkaido, Japan). Nano CS was produced by hydrolysis of the big CS using a subcritical water microreaction system (Yamada et al., 2013). High-purity big CS (H-big CS) and high-purity nano CS (H-nano CS, 6–14 sugar units) were respectively purified from the big and nano CSs using ethanol and activated charcoal treatments by Marukyo Bio Foods Co (purity 83.1 and 86.3%, respectively). These CSs were obtained as CS sodium salt. Thus, the big and nano CSs contained CS, minerals, and a small amount of peptides (≤10%). In contrast, the H-big- and H-nano CSs contained only CS and minerals. Pure chondroitin sulfate sodium salt from shark and bovine cartilage (shark CS and bovine CS) were purchased from Sigma-Aldrich (Saint Louis, MO; Lot BCBN1883V and Lot SLBR4195V, respectively). The compositions and MWts of skate, shark, and bovine CSs are summarized in Table 1.

Table 1

The formulations and molecular weights of CSs of different origins.

	Formulations (%)					Molecular weight (kDa)
	ΔDi-0s	ΔDi-4s (CS-A)	ΔDi-6s (CS-C)	ΔDi-2,6s (CS-D)	ΔDi-4,6s (CS-E)	
Big CS	6.5	26.6	60.9	6.5	0.1	10–250
Nano CS	10.8	8.5	71.9	8.8	n.d.	0.46–3.4
Shark CS	3.0	29.0	50.0	15.0	2.0	10–250
Bovine CS	6.0	61.0	33.0	n.d.	n.d.	10–40

Data of formulations for big CS and nano CS were obtained from Marukyo Bio Foods Co. Ltd, and for shark CS and bovine CS were obtained from the report of Volpi (2007). Data of molecular weights for big CS, shark CS, and bovine CS were obtained by 16.5% tricine-SDS-PAGE stained with Alcian blue. Data of molecular weight for nano CS was obtained from Marukyo Bio Foods Co. Ltd. n.d. = not detected.

2.2. In vitro *pancreatic lipase assay*

The lipase inhibitory activities of the CSs were quantified using a para-nitrophenyl phosphate (pNPP) assay, according to the method of Zhang et al. (2012), with minor modifications. In the assay, the pNPP was hydrolyzed by pancreatic lipase to release *para*-nitrophenol, a colored substance that can be quantified according to its absorbance at 405 nm. Lipase type II from porcine pancreas (Sigma-Aldrich) was dissolved in 50 mM Tris-HCl buffer (pH 8.0) at a concentration of 1.2 mg/ml and then centrifuged at 5,940 × *g* for 10 min to remove the insoluble components. The CSs were dissolved in deionized water at concentrations of 5 or 50 mg/ml. Orlistat (Sigma-Aldrich) is a lipase inhibitor that was used as a positive control. It was dissolved in DMSO at a concentration of 1,000 mM and then diluted in deionized water to a concentration of 100 mM.

Two types of reaction buffer were prepared. Reaction buffer 1 contained 50 mM Tris-HCl buffer (pH 8.0), 0.2% (w/v) sodium deoxycholate, 0.02% (w/v) lecithin (L-α-phosphatidylcholine, Sigma-Aldrich), and 5 mM $CaCl_2$. In Reaction buffer 2, 0.1% (w/v) gum arabic (Sigma-Aldrich) was used instead of the lecithin and $CaCl_2$. pNPP (Sigma-Aldrich) was dissolved in Reaction buffer at a concentration of 0.79 mM.

Lipase inhibitory activity was measured as follows. First, the reaction buffer (30 µl per well) and the pNPP solution (50 µl per well) were added to a 96-well microplate and pre-incubated for 10 min at 37°C. Simultaneously, the pNPP solution (650 µl per tube) and the CS solution (130 µl per tube) were mixed and pre-incubated. The reaction was started by adding 120 µl of the pNPP-CS mixture into each well, and then the plate was incubated at 37°C. After 30 min (reaction buffer 1) or 10 min (reaction buffer 2), the absorbance at 405 nm was measured using a microplate reader (Infinite F50R, Tecan Japan Co., Ltd., Kawasaki, Japan). Each experiment was carried out in triplicate.

The inhibition rate (%) was calculated using the following equation:

$$\text{Inhibition rate (\%)} = \left(1 - \frac{\mathrm{B} - \mathrm{b}}{\mathrm{A} - \mathrm{a}}\right) \times 100\%,$$

where A is an absorbance of the negative control (without sample but with lipase), a is the absorbance of the negative blank control (without sample and lipase), B is the experimental absorbance (with sample and lipase), and b is the absorbance of the experimental blank (with sample but without lipase).

176 *2.3. Endotoxin detection and reduction*

177

178 Endotoxin is composed of lipopolysaccharides that are contained in the outer
179 membrane of certain gram-negative bacteria, which are known to evoke an
180 inflammatory response by cells (Morris, Gilliam, Button, & Li, 2014). Therefore,
181 before the experiment, the endotoxin levels present in the CSs were reduced using an
182 EndotoxinOUT™ Kit (G-Bioscience, St. Lewis, MO). Briefly, freeze-dried CSs were
183 dissolved in endotoxin-free water (EFW) to 10 mg/ml, and a 1-ml sample was applied
184 to a kit column. After incubating at room temperature for 30 – 60 min, the sample was
185 eluted three times with 1 ml EFW. The eluate was then lyophilized and then the
186 recovery rate, which is the percentage of the dry masses of the sample before and after
187 the treatment, was calculated. The endotoxin levels in CSs were measured using a
188 *Limulus amebocyte* lysate (LAL) assay (ES-24S® Kit, lot No.24S16004; Seikagaku
189 Corp., Tokyo, Japan), according to the manufacturer's instructions. Control Standard
190 Endotoxin (CSE, Lot No.249025; Associates of Cape Cod Incorporated, E. Falmouth,
191 MA) was used as a standard.

192

193 *2.4. Cell culture experiment*

194

195 The mouse 3T3-L1 preadipocyte cell line was obtained from the RIKEN Cell
196 Bank (Tsukuba, Japan), and cultured in 96- or 48-well plates coated with 0.03%
197 porcine skin collagen (Cellmatrix type I-C, Nitta Gelatin Inc., Osaka, Japan) in an

198 atmosphere of 5% CO_2 at 37°C. First, cells were cultured in preadipocyte expansion
199 medium (Dulbecco's modified Eagle's medium containing high glucose [DMEM],
200 GIBCO, Grand Island, NY) containing 10% newborn calf serum (NCS, Lot 1751586;
201 GIBCO) and 1% penicillin/streptomycin (GIBCO). Two days after reaching
202 confluence, cells were induced to differentiate for 2 days in Differentiation medium
203 consisting of 1.0 μM dexamethasone (DEX, Sigma-Aldrich), 0.5 mM
204 3-isobutyl-1-methylxanthine (IBMX, Sigma-Aldrich), 1 μg/ml insulin
205 (Sigma-Aldrich), and 10% fetal bovine serum (FBS, Lot. No 451456, GIBCO) in
206 DMEM. Subsequently, the culture medium was changed to Adipocyte maintenance
207 medium consisting of DMEM, 10% FBS, and 1μg/ml insulin for 8 days. The
208 endotoxin-reduced CSs dissolved in EFW were added to the culture medium at
209 various concentrations and time points. EFW was used as a negative control.
210 Cell proliferation/metabolism was assessed using Cell Counting Kit-8 (CCK8,
211 Dojindo, Kumamoto, Japan), which measures total metabolic activity in the well, and
212 provides an estimate of total cell number if cellular metabolism is assumed to be
213 stable during the experiment. However, because we cannot be sure that cell
214 metabolism is not affected by the addition of CS, we use the terms "cell
215 number/metabolism" or "cell proliferation/metabolism" to denote this measurement in
216 this manuscript. After discarding the culture medium, 10% (v/v) CCK8 solution in
217 culture medium was added to each well, and following incubation at 37°C for 15 min,
218 the absorbance at 450 nm was measured using the microplate reader. Data are
219 expressed as the relative absorbance normalized to the absorbance of the control well.

Cellular triglyceride (TG) content was measured using a Triglyceride E-Test kit (Wako Pure Chemical Co., Osaka, Japan). After differentiation, cells in 48-well plates were washed twice with 0.1 M phosphate-buffered saline (PBS) and treated with trypsin-EDTA (GIBCO) until the majority of cells were floating in the medium. Cells were then collected by centrifugation and resuspended in PBS. The cell suspension was then frozen (−30°C, 30 min) and thawed (37°C, 30 min) three times and centrifuged to obtain the supernatant. Finally, the TG content of the supernatant was determined using the kit, and the absorbance was measured at 600 nm using the microplate reader.

Cellular morphology was examined under a microscope (DMI600B, Leica, Wetzlar, Germany) and photographed.

2.5. In vivo *experiment*

In vivo experiments were carried out at the New Drug Research Center Inc. (Eniwa, Hokkaido, Japan) and approved by the animal experiment committee of the New Drug Research Center Inc. (Permit Number 171030C). Four-week-old male C57B/6J mice (Charles River Laboratories Japan, Inc., Yokohama, Japan) were housed at a controlled environmental condition (22±3°C and 50±20% humidity) under a 12-12 h light-dark condition. The obesity model mice were established by feeding a high-fat diet (HFD) (60% kcal fat content, D12492, Research Diets Inc., New Brunswick, NJ). Following the acclimation for 7 days, mice were randomly divided into 3 groups (8

mice each): A-group mice were fed normal diet (ND) (D12450J, Research Diets Inc.) and orally administered 5 ml/kg/day distilled water; B-group mice were fed HFD and orally administered 5 ml/kg/day distilled water; C-group mice were fed HFD and orally administered 50 mg/5 ml/kg/day nano CS. Body weight was measured, and food consumption was calculated weekly for 8 weeks. After 8 weeks of treatment, feces were collected during the last 24 h. Blood samples were collected and centrifuged at 3000 rpm for 15 min, and then serum was obtained. After the mice were sacrificed, liver and adipose tissues (epididymal fat, perirenal and retroperitoneal fat, and mesenteric fat) were excised, weighted, and kept frozen at -70°C until analyses.

Total fat in feces and livers were extracted with chloroform-methanol-water (2:2:1), and the extracts were concentrated under a nitrogen stream. The triglyceride (TG) contents of the extracts and sera were determined using a Triglyceride E-Test kit (Wako Pure Chemical Co.). The endotoxin levels in the serum were estimated using ES-24S® Kit (Seikagaku Corp.).

2.6. Statistical analyses

Data are expressed as means ± standard errors. Statistical analyses were performed using Grubbs test for outliers, Student's *t*-test, the Tukey-Kramer test, and the Steel-Dwass test after ANOVA, in Microsoft Excel add-in statistical software (SSRI, Tokyo, Japan). Significance was set at $P<0.05$. The tendency was accepted at

264 $P<0.1$.

265

266 **3. Results and discussion**

267

268 *3.1. Effects of CSs on pancreatic lipase activity*

269

270 The CSs dose-dependently inhibited the hydrolysis of pNPP emulsified with
271 lecithin by pancreatic lipase (Fig. 1A). The inhibitory effects of the preparations were
272 also observed when the substrate pNPP was emulsified with gum arabic (Fig. 1B), but
273 the efficiency was lower than when lecithin was used as an emulsifier. These results
274 were similar to those obtained using salmon nasal cartilage CS (Han et al., 2000) and
275 suggest that our CSs also efficiently inhibit the interaction between the pancreatic
276 lipase and the substrate in the presence of lecithin. It is possible that when CSs bind to
277 the substrate, lecithin is likely to strengthen the binding as in the case of lipase
278 inhibitory action of chitosan (Han, Kimura, & Okuda, 1999), but gum arabic has no
279 such effects. A similar effect was also observed in the report of Han et al. (2000), in
280 which the lipase-inhibitory activity of salmon nasal CS is higher in lecithin-emulsified
281 experiments than in gum arabic-emulsified experiments.
282 The present assay, using lecithin as an emulsifier, also revealed that the skate big
283 CS yielded 50% inhibition of the pancreatic lipase activity at a concentration of 50
284 mg/ml but that its potency was significantly lower than those of shark and bovine CSs.
285 In addition, the skate big CS had a greater effect than skate nano CS at the same

concentration. These results imply that the inhibition of pancreatic lipase by CS depends on its origin and MWts. However, at 5 mg/ml the inhibitory activities were similar among all the CS preparations. High-purity nano CS also showed a dose-dependent inhibition of lipase (data not shown).

Orlistat, which showed the strongest inhibitory activity in the present lipase assay, is the only clinically approved drug for obesity treatment in Europe (Zhang & Lu, 2012). However, some adverse effects have been reported in patients undergoing orlistat therapy (Garza et al., 2011). Hence, CS preparations, including those derived from skate CS, may be candidates to replace orlistat as clinical inhibitors of pancreatic lipase.

In summary, lipase inhibition assays have shown that skate big CS is a natural inhibitor of pancreatic lipase and a candidate for inclusion in functional foods, which may have an impact in the intestinal tract. In addition to its potent lipase inhibitory activity, the low absorption of the big CS in the gut (Yamada et al., 2013) could further increase its usefulness. In contrast, the higher absorption of the nano CS would be expected in the gut (Yamada et al., 2013) and it was a less potent lipase inhibitor than big CS. We, therefore, evaluated the direct effects of nano CS on adipocyte metabolism using a cell culture system.

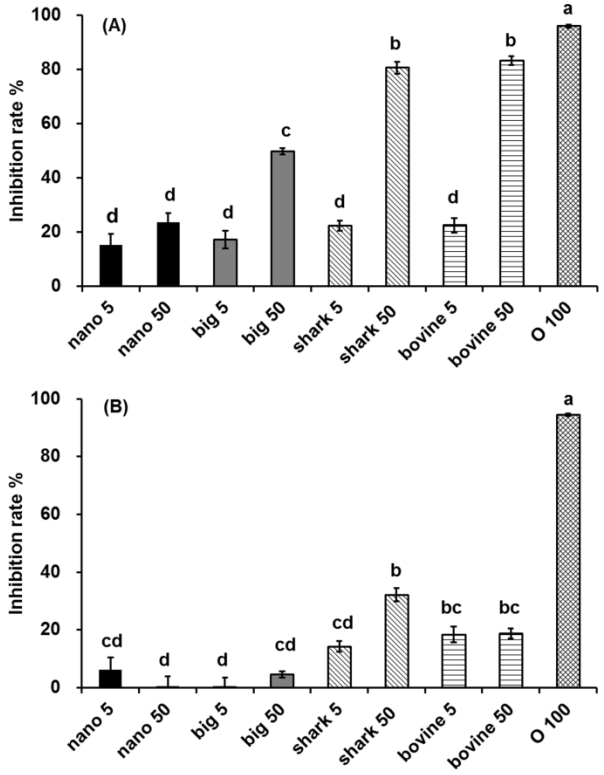

Fig.1. Effects of CSs on pancreatic lipase activity. (A) pNPP emulsified with lecithin was used as a substrate. The reaction time was 30 min. (B) pNPP emulsified with gum arabic was used as a substrate. The reaction time was 10 min. The columns and vertical bars show the mean values and standard errors, respectively (n=3). Different letters indicate statistical difference ($p < 0.05$). Nano 5, nano CS 5 mg/ml; nano 50, nano CS 50 mg/ml; big 5, big CS 5 mg/ml; big 50, big CS 50 mg/ml; shark 5, shark CS 5 mg/ml; shark 50, shark CS 50 mg/ml; bovine 5, bovine CS 5 mg/ml; bovine 50, bovine CS 50 mg/ml; O 100, orlistat 100 mM.

3.2. Endotoxin levels of CSs after endotoxin-reduction treatment

The endotoxin content of the CSs before and after the endotoxin-reduction treatment is shown in Table 2. The CSs of different origins had contrasting endotoxin contents, which may relate to the methods of production and purification used for each. The endotoxin levels of the H-nano and H-big CSs were low, suggesting that the purification with ethanol and activated carbon had an endotoxin-reducing effect.

After the endotoxin-reduction chromatography, the recovery rates for the CSs

were more than 75%. Their endotoxin levels were significantly lower after the treatment, becoming < 0.4 ng/mg. A low concentration of LPS (≤ 1 ng/ml) did not induce the production of the inflammatory mediators, interleukin (IL)-6, tumor necrosis factor α, and IL-33, in human monocytic cells (Morris et al., 2014). Because the maximum concentration of CS used in the present cell culture experiment was 1 mg/ml, we judged that all CSs were suitable for use in cell culture experiments after the endotoxin-reduction step. The endotoxin level of the nano CS was reduced by 97.6% by the treatment, which was a much greater reduction than was achieved with the other CSs. This might be because nano CS has a simpler structure, higher solubility in water, and lower viscosity.

Table 2

The endotoxin levels present in CSs before and after the endotoxin-reduction treatment.

	Endotoxin levels ng/mg (EU/mg)	
	Before the treatment	After the treatment
Nano CS	1.67 (13.36)	0.04 (0.32)
Big CS	2.67 (21.36)	0.40 (3.20)
Shark CS	3.63 (29.04)	0.38 (3.12)
Bovine CS	0.33 (2.64)	0.10 (0.80)
H-nano CS	0.01 (0.08)	-
H-big CS	0.15 (1.20)	0.06 (0.48)

- : no data (no need for endotoxin-reduction treatment).

The potency of the standard endotoxin used in the experiment was 8 EU/ng.

3.3. Effect of CSs on 3T3-L1 proliferation/metabolism

To compare the effects of CSs on adipocytes, high-purity samples (H-nano, H-big, shark, and bovine CSs) were used in cell culture experiments.

First, 3T3-L1 preadipocytes were treated with H-nano CS at various concentrations (10, 100, or 1,000 μg/ml) during the preadipocyte expansion period (Days 1–8) and the cell number/metabolism was estimated using CCK8 (Figs. 2A–C). In addition, CS polysaccharides of various origins were tested at 1,000 μg/ml. During Days 3–8, no significant effects of H-nano CS were observed on cell proliferation/metabolism, except for a small difference at a dose of 100 μg/ml on Day 3. In contrast, H-big and shark CS significantly enhanced 3T3-L1 preadipocyte proliferation/metabolism. These data indicate that skate and shark CS-polysaccharides accelerate preadipocyte proliferation/metabolism, but CS oligosaccharides and bovine CS do not. The explanation could be that the formulation of the bovine CS is different from that of the skate and shark preparations (Table 1). Nevertheless, these data suggest that the effect of CSs on preadipocyte proliferation/metabolism depends on their origin and MWts.

Next, the CSs were added to the culture during the adipocyte differentiation and maintenance periods. CCK8 assays were conducted at the end of the 2-day differentiation period (the start of the maintenance period) and at the end of the 8-day maintenance period (Fig. 3). During the differentiation period, 1,000 μg/ml H-big CS significantly increased preadipocyte number/metabolism over that of the EFW control group. However, a significant difference was not induced by the addition of other CSs.

During the adipocyte maintenance period, the number/metabolism of cells in the EFW group remained constant. In contrast, there was a downward trend in the number/metabolism of cells during the maintenance period in all CS-treated groups. At the end of the maintenance period, the number/metabolism of cells in wells treated with 1,000 μg/ml H-nano CS, H-big CS, shark CS, or bovine CS was significantly lower than at the beginning of this period.

These data indicate that the CSs have differing effects on cell proliferation/metabolism, depending on the differentiation stage of the adipocytes: they tend to enhance the proliferation/metabolism of preadipocytes but suppress the number/metabolism of differentiated adipocytes. Two previous studies of the anti-obesity actions of CSs (2000; Xu et al., 2015) did not investigate the effects of CSs on the proliferation of adipocytes. Therefore, to our knowledge, this is the first report of the effects of CSs on the proliferation of adipogenic cells.

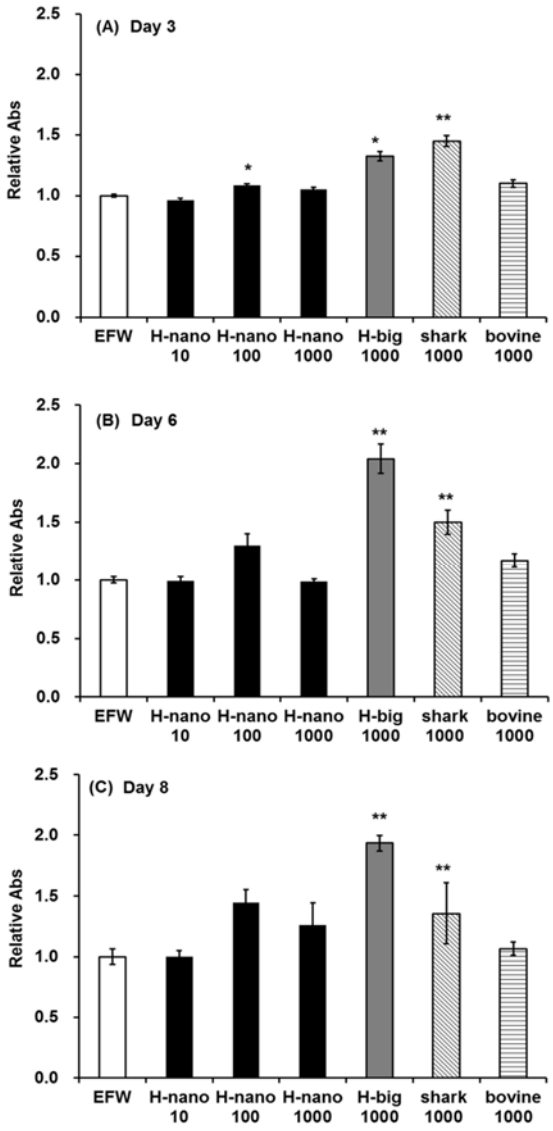

Fig.2. Effect of CSs on 3T3-L1 proliferation. Values are expressed relative to the corresponding EFW control. The columns and bars show the mean values and standard errors, respectively (n=10). * $p < 0.05$ and ** $p < 0.01$ compared with the control group (EFW). EFW, endotoxin-free water; H-nano 10, H-nano CS 10 μg/ml; H-nano 100, H-nano CS 100 μg/ml; H-nano 1000, H-nano CS 1,000 μg/ml; H-big 1000, H-big CS 1,000 μg/ml; shark 1000, shark CS 1,000 μg/ml; bovine 1000, bovine 1,000 μg/ml.

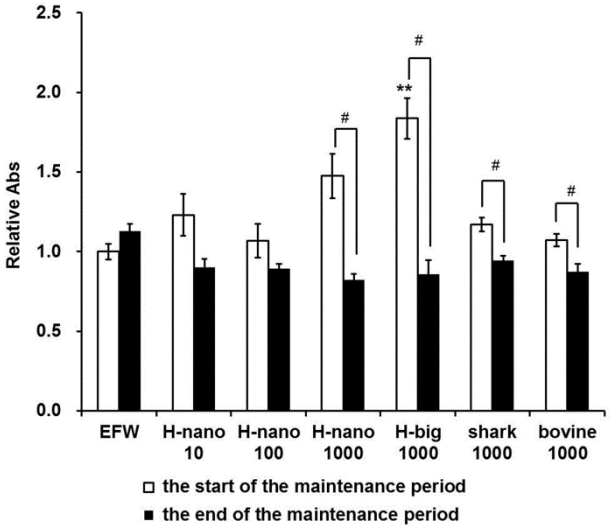

Fig.3. Effect of CSs on 3T3-L1 adipocyte proliferation during the adipocyte maintenance period. Two days after the cells reached confluence, they were treated to induce their differentiation into mature adipocytes. After 2 days (at the start of the maintenance period), the culture medium was changed to Adipocyte maintenance medium, and the cells were cultured for a further 8 days. Values are expressed relative to their corresponding EFW control at the start of the maintenance period. The columns and bars show the mean values and standard errors, respectively (n=10). ** p <0.01 compared with the control group (EFW) (Steel-Dwass test) and # p < 0.01 compared with the start of the maintenance period (Student's t-test).

3.4. Effect of CSs on lipid accumulation in 3T3-L1 adipocytes

CSs were added to cultures during the adipocyte differentiation and maintenance periods to evaluate their effects on lipid accumulation, with adipocyte TG content being measured at the end of the maintenance period. As shown in Fig. 4, all CSs tended to inhibit lipid accumulation when compared with the EFW control wells. H-nano CS significantly reduced TG content when added at 10 μg/ml, and both H-big and shark CSs significantly reduced TG content at higher concentrations. In particular, the lipid content of cells treated with shark CS at 1,000 μg/ml was below the detection limit. However, the inhibitory effect of bovine CS was weaker: the TG content in

419 bovine CS-treated cells was not significantly different from the control, suggesting
420 that the effect of CS to inhibit lipid accumulation depends on its origin.
421 It has been previously reported that glucagon-like peptide 1 affects lipid droplet
422 size and number in 3T3-L1 cells (Yang et al., 2013). The lipid droplet size in 1,000
423 μg/ml H-nano-treated cells was smaller than that of control cells (Fig. 5). These data
424 indicate that high concentrations of H-nano inhibit the development of lipid droplets
425 in differentiating adipocytes. Also, larger spaces can be observed between adipocytes
426 in cells treated with 1,000 μg/ml H-nano CS (Fig. 5). These larger spaces could be the
427 result of reductions in cell number during the maintenance period, consistent with the
428 CCK8 data. Therefore, skate CS oligosaccharides have inhibitory effects on mature
429 adipocytes.
430 In contrast to the cell morphology observed following the treatment of cells with
431 other types of CS, spindle-shaped cells without lipid droplets were observed in cells
432 treated with 1,000 μg/ml H-big CS (Fig. 5), accompanied by a clear separation
433 between cells. Such morphological characteristics are shared with undifferentiated
434 preadipocytes. These data suggest that H-big CS inhibits adipocyte differentiation and
435 causes changes in cell morphology, while H-nano CS affects lipid droplet
436 accumulation in maturing adipocytes. Therefore, the mechanisms suppressing
437 differentiation of 3T3-L1 adipocytes depend on the MWts of the skate CS. These
438 results also explain the contrasting effects of similar doses of H-nano and H-big CSs
439 on cell morphology. When preadipocytes differentiate into adipocytes, the synthesis
440 and secretion of proteoglycans create a loose extracellular space between cells (Calvo,

441 Rodbard, Katki, Chernick, & Yanagishita, 1991). Because CS is a major component of
442 proteoglycans, the addition of H-big CS (more than 50 sugar units) may provide a
443 negative feedback signal to suppress the differentiation of adipocytes. However,
444 H-nano CS (6–14 sugar units) may not have the same effect. Presently, the
445 mechanisms of H-nano CS to reduce lipid droplets are unknown. Our working
446 hypothesis is that H-nano CS binds to cell surface receptor, such as Toll-like receptor
447 2, to inhibit related-gene PPARγ expression, and then inhibit lipid accumulation in
448 mature adipocytes (Wu et al, 2018; Wahli & Michalik, 2012; Xu et al., 2015). The
449 mechanism will be investigated in the future.

450 In summary, 3T3-L1 culture experiments revealed that skate CS inhibits
451 proliferation/metabolism of maturing adipocytes and reduces the accumulation of
452 lipid droplets, although in contrast it activates preadipocyte proliferation/metabolism
453 at higher concentrations. Although both H-big CS, H-nano CS, and shark CS inhibit
454 lipid accumulation, H-nano CS would be more appropriate for oral administration,
455 because it passes through the digestive system more readily (Yamada et al., 2013;
456 Wang, Zhang, & Jin, 2016). Moreover, H-nano CS has higher water solubility and
457 lower viscosity. Taken together, our findings suggest that H-nano CS could be an
458 appropriate material for inclusion in anti-obesity functional foods.

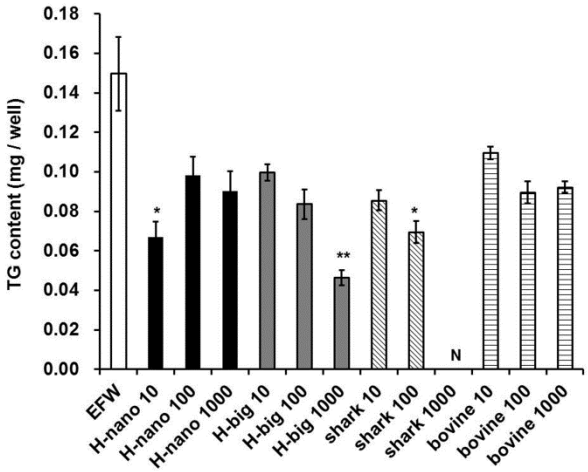

Fig.4. Effect of CSs on lipid accumulation in 3T3-L1 adipocytes. The columns and bars show the mean values and standard errors, respectively (n=3). * $p < 0.05$ and ** $p < 0.01$ compared with the EFW control. N, below detection limit; EFW, endotoxin-free water; H-nano 10, H-nano CS 10 μg/ml; H-nano100, H-nano CS 100 μg/ml; H-nano 1000, H-nano CS 1,000 μg/ml; H-big 10, H-big CS 10 μg/ml; H-big 100, H-big CS 100 μg/ml; H-big 1000, H-big CS 1,000 μg/ml; shark 10, shark CS 10 μg/ml; shark 100, shark CS 100 μg/ml; shark 1000, shark CS 1,000 μg/ml; bovine 10, bovine 10 CS μg/ml; bovine 100, bovine CS 100 μg/ml; bovine 1000, bovine CS 1,000 μg/ml.

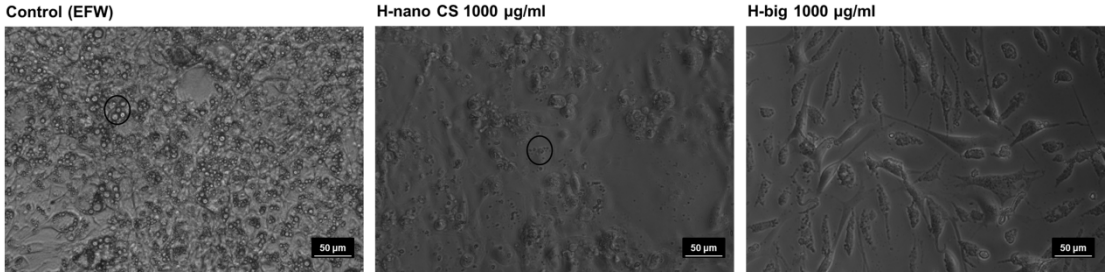

Fig.5. Effect of H-nano CS and H-big CS on 3T3-L1 adipocyte morphology and lipid droplets. Photomicrographs of 3T3-L1 adipocytes at the end of the culture period. Lipid droplets were observed by phase contrast microscopy. Circle, lipid droplets. Bars, 50 μm.

3.5. In vivo *effect of nano CS*

The anti-obesity effects of nano CS were studied using animal experiments. In this experiment, one mouse in C group (HFD with nano CS 50 mg/kg) was excluded as an outlier because its growth rate was extremely high (Grubbs test for outliers, $P < 0.01$).

As shown in Fig. 6A, consumption of HFD for 8 weeks (B group) showed a significant gain of body weight compared with A group (fed ND). In contrast, the body weight of mice in the C group was at the same level as A group during the early stage (weeks 1-5). After 5 weeks, the body weight of mice in C group was higher than A group but significantly lower than the B group, indicating that nano CS prevented weight gain when mice were fed HFD.

From the results of Fig. 6B, HFD decreased food consumption per week at the early stage in both B and C groups. From 5 weeks, however, the B-group mice returned to the normal level of food consumption. The C-group mice also returned their appetite except for the significantly lower food consumption on week 7 compared with A group. There was no significant difference in food consumption between group B and C at any time point.

As shown in Table 3, HFD caused mice to increase the weight of adipose tissues. HFD also increased the total TG content of the liver and feces. Compared with the B group, however, C group shows significantly lower liver weight with a decreasing tendency of total TG content of the liver. At the same time, adipose tissues around the kidney and posterior abdominal in C-group mice also showed a decreasing trend than the B group. Serum TG concentrations among the three groups were not significantly different. These results suggest that CS slows down the accumulation of lipids induced by HFD, supporting the results of our adipocyte-culture experiments. In addition, the total TG content of feces in C group was tended to increase compared with B group, suggesting that nano CS inhibited the absorption of TG, which is in line

501 with its lipase-inhibitory activity.

502 Obesity leads to metabolic disorders and chronic inflammation. High endotoxin
503 level in plasma is a marker of metabolic endotoxemia and inflammatory disorders,
504 which relate with liver lipogenesis, insulin sensitivity and so on (Cani et al., 2009).
505 Our mouse experiment (Table 3) showed that the serum endotoxin levels of the B
506 group were significantly higher than A group. Oral administration of nano CS
507 inhibited HFD-induced hyperendotoxemia: the serum endotoxin level of C group was
508 statistically similar levels with A group. This result indicated that nano CS could help
509 to adjust metabolism and inflammatory disorders induced by HFD.

510 As a whole, skate CS oligosaccharides can ameliorate obesity in HFD-induced
511 obese mice through inhibition of lipid absorption and accumulation.

512 To the best of our knowledge, the anti-obesity effects of CS have only been
513 reported for salmon nasal CS (Han et al., 2000) and fucosylated CS of sea cucumber
514 (Xu et al., 2015; Li et al., 2018). CS from salmon nasal cartilage inhibited lipase
515 activity, and its oral administration evoked a significant reduction in body weight and
516 parametrial adipose tissue mass (Han et al., 2000). However, any direct effect of
517 salmon CS on adipocytes has not been established. Since the salmon nasal cartilage
518 CS has high MWts (89.8 kDa) (Han et al., 2000), its intestinal absorbability must be
519 low; and thus, the major mechanism of anti-obesity action of salmon nasal cartilage
520 CS is supposed to be inhibition of intestinal lipid absorption. In fucosylated CS
521 (average MWts: 21.53 kDa), anti-adipogenic effects on cultured adipocytes and
522 anti-obesity effects on high-fat-high-sucrose diet mice were shown (Xu et al., 2015).

Also, the anti-obesity action of depolymerized fucosylated CS (MWts: 4.3 kDa) in high-fat diet mice was shown recently (Li et al., 2018). The fucosylated CS, however, has chondroitin sulfate E backbone with fucose branches, which is different from CSs from vertebrates. So, this study is the first to certify the *in vitro* anti-adipogenic and *in vivo* anti-obesity effects of vertebrate-type CS oligosaccharides with high intestinal absorbability.

This study is also the first to demonstrate the contrasting effects of skate CSs of differing MWts at various time points. CS-polysaccharides, which are not significantly absorbed from the intestine, showed stronger inhibition of intestinal lipid digestion, whereas CS-oligosaccharides, which are more readily absorbed, inhibited lipid accumulation by adipocytes at lower concentrations. This is noteworthy because the skate CSs with different MWts could be used for different purposes: high MWt CS as an inhibitor of pancreatic lipase in the intestine and CS oligosaccharides as inhibitors of lipid accumulation in differentiating adipocytes. Therefore, a combined preparation of both types may be effective as an anti-obesity functional food.

Moreover, this is the first report regarding the differing potency of CSs from different species. To the best of our knowledge, skate (H-big) and shark CSs are similarly formulated, but the formulation of bovine CS differs (Table 1). Our data show similar effects of skate and shark CS on preadipocyte proliferation and adipocyte lipid accumulation, which is in accordance with their similar formulation. It is well known that CSs that are formulated differently have differing bioactivities. For example, some CSs have anti-inflammatory effects, while others have weaker effects,

and others are pro-inflammatory (Martelpelletier et al., 2015). In addition, the specific effect of H-big CS on the morphology of the 3T3-L1 cells may relate to its high proportion of non-sulfated and mono-sulfated disaccharides and its lower proportion of di-sulfated disaccharides compared with other CSs. Because CSs of different origins have distinct formulations and structures, further comparative studies are needed to understand the relationships between CS structure and biological potency.

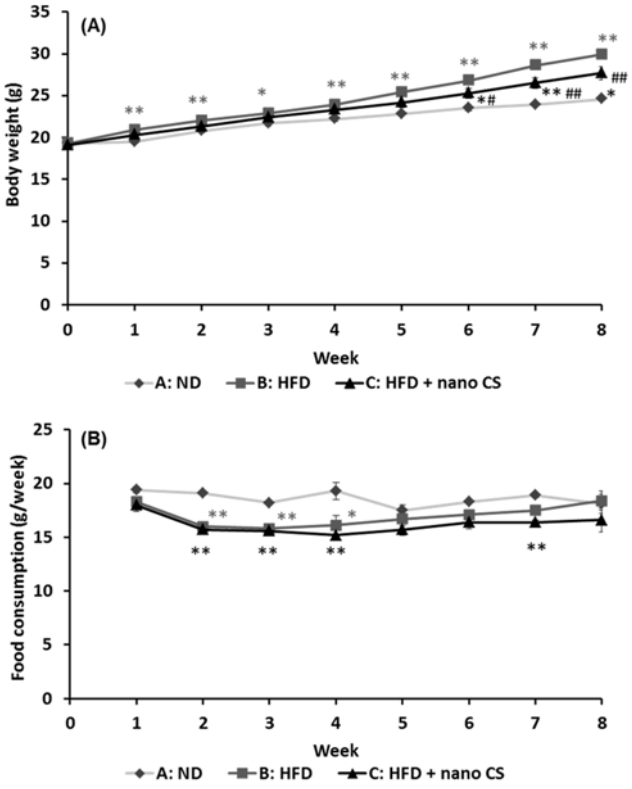

Fig.6. Effect of nano CS on body weight (A) and food consumption (B) in HFD fed mice model. The date and bars show the mean values and standard errors, respectively (n=7 or 8). * $p < 0.05$ and ** $p < 0.01$ compared with A group. # $p < 0.05$ and ## $p < 0.01$ indicate significant difference between B and C groups.

559 **Table 3**

560 The effect of nano CS on tissues wet weight, total TG content, and endotoxin level in the HFD fed

561 mice model.

		A: ND + DW	B: HFD + DW	C: HFD + nano CS in DW
Tissues wet weight (g/individual)	Liver	0.9332 ±0.0191	0.9883±0.0153	0.9041±0.0219$^{\#}$
	Epididymal fat	0.4603±0.0221	1.5500±0.0304**	1.2725±0.1197**
	Perirenal and retroperitoneal fat	0.1274±0.0159	0.5953±0.0116**	0.4680±0.0475**†
	Mesenteric fat	0.1922±0.0215	0.3560±0.0191**	0.3314±0.0401**
Total TG (mg)	Liver	0.0069±0.0008	0.0128±0.0009**	0.0101±0.0007*†
	Feces	0.0010±0.0003	0.0018±0.0001	0.0026±0.0004*†
Serum TG concentration (mg/dl)		73.5±7.6	82.4±3.0	73.3±3.5
Serum endotoxin level (pg/ml)		46.00±1.70	55.30±1.51**	51.70±1.89

562 Data are expressed as mean ± standard errors (n=7 or 8). *$p < 0.05$ and **$p < 0.01$ compared with

563 A group. #$p < 0.05$ compared with B group. †$p < 0.1$ shows tendency of decrease in C group

564 compared with B group.

565

566 ## 4. Conclusion

567 This study clearly demonstrates the anti-obesity effects of skate CS

568 oligosaccharides *in vitro* and *in vivo*. Skate CS oligosaccharides have a

569 lipase-inhibitory activity to inhibit the absorption of TG in the intestine and have an

570 adipocyte-inhibitory activity to reduce lipid accumulation. It can control weight gain

571 and adjust metabolic disorders in HFD mice. The MWt of the CS affected the skate

572 CS mode of action: high MWt CS (CS polysaccharides), which cannot be intestinally

573 absorbed, had stronger lipase inhibitory activity, which would be expected to inhibit

574 dietary fat absorption in the intestine, whereas low MWt CS (CS oligosaccharides),

575 which are more readily absorbed, suppressed adipocyte lipid accumulation at a lower
576 dose. These results suggest that a formulation containing both CSs may be effective as
577 an anti-obesity functional food. Also, the present study has shown that CS
578 preparations all inhibit lipase, but their potency depends on their origin, as does their
579 effect on adipocytes. Thus, the origin of CS is a key factor in its bioactivity.
580
581 **Acknowledgments**
582
583 We thank Mark Cleasby, Ph.D., from Edanz Group (www.edanzediting.com/ac) for
584 editing a draft of this manuscript. This study was supported in part by Grants-in-Aid
585 for the Regional R&D Proposal-Based Program (H28 SL-2-2) from the Northern
586 Advancement Center for Science & Technology of Hokkaido Japan.
587
588 **Declaration of interest: none.**
589 **References**
590
591 Calvo, J. C., Rodbard, D., Katki, A., Chernick, S., & Yanagishita, M. (1991).
592 Differentiation of 3T3-L1 preadipocytes with 3-isobutyl-1-methylxanthine and
593 dexamethasone stimulates cell-associated and soluble chondroitin 4-sulfate
594 proteoglycans. *Journal of Biological Chemistry, 266(17)*, 11237-11244.
595 Cani P. D., Possemiers S., Van de Wiele T., Guiot Y., Everard A., Rottier O., Geurts L.,
596 Naslain D., Neyrinck A., Lambert D. M., Muccioli G. G., & Delzenne1 N. M.

(2009). Changes in gut microbiota control inflammation in obese mice through a mechanism involving GLP-2-driven improvement of gut permeability. *Gut, 58,* 1091–1103.

FAO. International Plan of Action for Conservation and Management of Sharks. (2014). http://www.fao.org/ipoa-sharks/background/sharks/en/.

Garza, A. L., Milagro. F., Boque N., Campión. J., Martínez. J. (2011). Natural inhibitors of pancreatic lipase as new players in obesity treatment. *Planta Medica*, *77*, 773-785.

Han, L. K., Kimura, Y., & Okuda, H. (1999). Reduction in fat storage during chitin-chitosan treatment in mice fed a high-fat diet. *International Journal of Obesity*, *23(2)*, 174.

Han, L. K., Sumiyoshi, M., Takeda, T., Chihara, H., Nishikiori, T., Tsujita, T., Kimura, Y., & Okuda, H. (2000). Inhibitory effects of chondroitin sulfate prepared from salmon nasal cartilage on fat storage in mice fed a high-fat diet. *International Journal of Obesity*, *24*, 1131-1138.

Hashiguchi, T., Kobayashi, T., Fongmoon, D., Shetty, A. K., Mizumoto, S., Miyamoto, N., Nakamura, T., Yamada, S., & Sugahara, K. (2011). Demonstration of the hepatocyte growth factor signaling pathway in the in vitro neuritogenic activity of chondroitin sulfate from ray fish cartilage. *Biochimica et Biophysica Acta*, *1810*, 406-413.

Kobayashi, T., Kakizaki, I., Nozaka, H., & Nakamura, T. (2017). Chondroitin sulfate proteoglycans from salmon nasal cartilage inhibit angiogenesis. Biochemistry &

619 *Biophysics Reports*, *9*, 72-78.
620 Kwok, J. C. F., Warren, P., & Fawcett, J. W. (2012). Chondroitin sulfate: a key
621 molecule in the brain matrix. *International Journal of Biochemistry & Cell*
622 *Biology*, *44*, 582-586.
623 Li, S., Li, J., Mao, G., Hu, Y., Ye, X., Tian, D., Linhardt, R.J., & Chen, S. (2018).
624 Fucosylated chondroitin sulfate oligosaccharides from *Isostichopus badionotus*
625 regulates lipid disorder in C57BL/6 mice fed a high-fat diet. *Carbohydrate*
626 *Polymers*, *201*, 634-642.
627 Martelpelletier, J., Farran, A., Montell, E., Vergés, J., & Pelletier, J. P. (2015).
628 Discrepancies in composition and biological effects of different formulations of
629 chondroitin sulfate. *Molecules*, *20*, 4277-4289.
630 Melgar-Lesmes, P., Garcia-Polite, F., Del-Rey-Puech, P., Rosas, E., Dreyfuss, J. L.,
631 Montell, E., Montell, E., Vergés, J., Edelman, E. R., & Balcells M. (2015).
632 Treatment with chondroitin sulfate to modulate inflammation and atherogenesis
633 in obesity. *Atherosclerosis*, *245*, 82-87.
634 Morris, M. C., Gilliam, E. A., Button, J., & Li, L. (2014). Dynamic modulation of
635 innate immune response by varying dosages of lipopolysaccharide (LPS) in
636 human monocytic cells. *Journal of Biological Chemistry*, *289*, 1-11.
637 Murado, M. A., Fraguas, J., Montemayor, M. I., Vázquez, J. A., & González, P. (2010).
638 Preparation of highly purified chondroitin sulphate from skate (*Raja clavata*)
639 cartilage by-products. *Biochemical Engineering Journal*, *49*, 126-132.
640 Volpi, N. (2007). Analytical aspects of pharmaceutical grade chondroitin sulfates.

641 *Journal of Pharmaceutical Sciences*, *96*, 3168-3181.
642 Wang, J., Zhang, L., & Jin, Z. (2016). Separation and purification of
643 low-molecular-weight chondroitin sulfates and their anti-oxidant properties.
644 *Bangladesh Journal of Pharmacology*, *11*, 61-67.
645 Wahli, W., & Michalik, L. (2012). PPARs at the crossroads of lipid signaling and
646 inflammation. *Trends in Endocrinology & Metabolism*, *23(7)*, 351-363.
647 Wu, F., Zhou, C., Zhou, D., Ou, S., Liu, Z., & Huang, H. (2018). Immune-enhancing
648 activities of chondroitin sulfate in murine macrophage RAW 264.7 cells.
649 *Carbohydrate Polymers*, *168*, 611-619.
650 Xu, H., Wang, J., Zhang, X., Li, Z., Wang, Y., & Xue, C. (2015) Inhibitory effect of
651 fucosylated chondroitin sulfate from the sea cucumber *Acaudina molpadioides*,
652 on adipogenesis is dependent on Wnt/β-catenin pathway. *Journal of Bioscience*
653 *& Bioengineering*, *119*, 85-91.
654 Yamada, S., Matsushima, K., Ura, H., Miyamoto, N., & Sugahara, K. (2013). Mass
655 preparation of oligosaccharides by the hydrolysis of chondroitin sulfate
656 polysaccharides with a subcritical water microreaction system. *Carbohydrate*
657 *Research*, *371C (8)*, 16-21.
658 Yang, J., Ren, J., Song, J., Liu, F., Wu, C., Wang, X., Gong, L., Li, W., Xiao, F., Yan,
659 F., & Chen, L., (2013). Glucagon-like peptide 1 regulates adipogenesis in
660 3T3-L1 preadipocytes. *International Journal of Molecular Medicine*, *31*,
661 1429-1435.
662 Zhang, L., & Lu, Y. (2012). Inhibitory activities of extracts from *Cleistocalyx*

663 *operculatus* flower buds on pancreatic lipase and α-amylase. *European Food*
664 *Research and Technology*, *235*, 1133-1139.
665